NEOPLASIA
www.neoplasia.com

Volume 18 Number 9 September 2016 pp. 525–535 525

Induction of Activating Transcription Factor 3 Is Associated with Cisplatin Responsiveness in Non–Small Cell Lung Carcinoma Cells[1,2]

Jair Bar*,¶,3, Mohamed S. Hasim*,‡,3, Tabassom Baghai*,3, Nima Niknejad*, Theodore J. Perkins†,‡,§, David J. Stewart¶, Harmanjatinder S. Sekhon#, Patrick J. Villeneuve*, and Jim Dimitroulakos*,‡**

*Centre for Cancer Therapeutics, Ottawa Hospital Research Institute, Ottawa, Ontario, Canada; †Regenerative Medicine, Ottawa Hospital Research Institute, Ottawa, Ontario, Canada; ‡Faculty of Medicine, Department of Biochemistry, Microbiology and Immunology, Ottawa, Ontario, Canada; §Cellular and Molecular Medicine, University of Ottawa, Ottawa, Ontario, Canada; ¶Department of Medical Oncology, the Ottawa Hospital, Ottawa, Ontario, Canada; #Department of Anatomical Pathology, the Ottawa Hospital, Ottawa, Ontario, Canada; **Department of Thoracic Surgery, the Ottawa Hospital, Ottawa, Ontario, Canada

Abstract

Non–small cell lung carcinoma (NSCLC) is the most common cause of cancer deaths, with platin-based combination chemotherapy the most efficacious therapies. Gains in overall survival are modest, highlighting the need for novel therapeutic approaches including the development of next-generation platin combination regimens. The goal of this study was to identify novel regulators of platin-induced cytotoxicity as potential therapeutic targets to further enhance platin cytotoxicity. Employing RNA-seq transcriptome analysis comparing two parental NSCLC cell lines Calu6 and H23 to their cisplatin-resistant sublines, Calu6cisR1 and H23cisR1, activating transcription factor 3 (ATF3) was robustly induced in cisplatin-treated parental sensitive cell lines but not their resistant sublines, and in three of six tumors evaluated, but not in their corresponding normal adjacent lung tissue (0/6). Cisplatin-induced JNK activation was a key regulator of this ATF3 induction. Interestingly, in both resistant sublines, this JNK induction was abrogated, and the expression of an activated JNK construct in these cells enhanced both cisplatin-induced cytotoxicity and ATF3 induction. An FDA-approved drug compound screen was employed to identify enhancers of cisplatin cytotoxicity that were dependent on ATF3 gene expression. Vorinostat, a histone deacetylase inhibitor, was identified in this screen and demonstrated synergistic cytotoxicity with cisplatin in both the parental Calu6 and H23 cell lines and importantly in their resistant sublines as well that was dependent on ATF3 expression. Thus, we have identified ATF3 as an important regulator of cisplatin cytotoxicity and that ATF3 inducers in combination with platins are a potential novel therapeutic approach for NSCLC.

Neoplasia (2016) 18, 525–535

Address all correspondence to: Jim Dimitroulakos, Centre for Cancer Therapeutics, Ottawa Hospital Research Institute, 501 Smyth Road, Box 926, Ottawa, Ontario, K1H 8L6.
E-mail: jdimitroulakos@ohri.ca

[1] Grant support: Funding support from the Cancer Research Society (20120106), Canadian Institute for Health Research (IC1-123782), the Lung Cancer Research Foundation (20120877), the Joan Sealy Trust and the Prostate Cancer Fight Foundation is greatly appreciated.

[2] Disclosure of potential conflicts of interest: No potential conflicts of interest were disclosed.
[3] Contributed equally to this work.
Received 2 April 2016; Revised 30 June 2016; Accepted 11 July 2016

1476-5586
http://dx.doi.org/10.1016/j.neo.2016.07.004

Introduction

Lung cancer, predominantly non–small cell lung cancer (NSCLC), is the most common cause of cancer death, surpassing the next five most common causes combined [1]. Platins, particularly cisplatin and carboplatin, are the most active agents in NSCLC [2], and platin-based chemotherapy combinations are typically the first-line therapy in the advanced (metastatic) setting [3]. However, the overall gains in survival have been modest, with a median survival of approximately 12 months in patients receiving platin doublet chemotherapy compared to 4 months in untreated patients [4]. Approximately 30% of patients will show antitumor responses, but these responses are not durable, with treatments resulting in a relatively modest effect on overall patient survival [5]. Identification of novel therapeutic approaches including next-generation platin combination strategies is urgently required.

Although platin-induced cytotoxicity results from DNA damage that drives their cytotoxicity, the mechanisms and cellular pathways underlying the proapoptotic effect of these chemotherapeutic agents are largely undefined [6]. Understanding the mechanisms regulating tumor cell cytotoxicity may uncover novel therapeutic strategies to enhance the efficacy of these platin-based chemotherapeutics. Cisplatin and carboplatin are primarily considered to be DNA-damaging anticancer drugs forming different types of adducts in reaction with cellular DNA [2]. The final cellular outcome of DNA adduct formation is generally apoptotic cell death, and multifactorial cellular mechanisms of resistance to platin-based chemotherapeutics include apoptosis inhibition [6]. DNA is the recognized primary target of cisplatin and carboplatin activity [7], but gaps still remain in our understanding of the process that translates cisplatin-induced DNA damage into its therapeutically beneficial process of apoptosis. Two significant cellular pathways have been demonstrated to play key roles in platin-induced apoptosis/cytotoxicity: the mitogen-activated protein kinase cascades (MAPKinase) and the tumor suppressor p53 [8,9].

There is significant interest in the role of MAPKinase pathways in platin's mode of action. The major MAPK subfamily members include the extracellular signal–regulated kinases (ERK), the c-Jun N-terminal kinases (JNK), and the p38 kinases [10,11]. A number of studies have demonstrated that all three kinase members can be activated following exposure of tumor cells to cisplatin and play a role in regulating cisplatin-induced apoptosis [12,13]. However, the downstream targets of these pathways have not been well characterized. Employing RNA-seq transcriptome analysis, we identified a known MAPKinase-induced cellular stress pathway, highlighted by activating transcription factor 3 (ATF3) [14,15], which was specifically induced by cisplatin in sensitive but not resistant cells and was a key regulator of cisplatin-induced cytotoxicity and resistance. Elevated and sustained levels of stress-induced ATF3 enhance apoptosis, suggesting that ATF3 inducers may enhance the cytotoxic activity of platins, representing a potentially novel and rational therapeutic approach.

Materials and Methods

Tissue Culture

The human NSCLC tumor–derived cell lines Calu6 and NCI-H23 (H23), the breast cancer cell lines MCF7 and T47D, and the prostate cancer cell lines LNCAP and PC3 were obtained from the ATCC (Rockville, MD, USA). The murine embryonic fibroblasts (MEFs) ATF3−/− deficient in ATF3 expression through gene knockout and their wild-type counterparts were kindly provided by Dr. T. Hai, (Ohio State University, Columbus, OH). Cells were maintained in Dulbecco's modified Eagle's medium (Media Services, Ottawa Regional Cancer Centre) supplemented with 10% fetal bovine serum (Medicorp, Montreal, QC, Canada). To derive cisplatin-resistant Calu6 and H23 sublines (designated cisR), cells were plated and treated with 2 μg/ml cisplatin until a surviving fraction of about 10^{-6} remained [16]. Following this cisplatin treatment regimen, sublines isolated from single cells were propagated. Cisplatin, carboplatin, doxorubicin, and docetaxel were provided by the pharmacy at the Ottawa Hospital Cancer Centre, Ottawa. For JNK expression experiments, Calu6cisR1 cells plated at 3×10^5 in 6-well plates were transfected with 2 μg of a JNK1a1-expressing plasmid (Addgene, Plasmid #13,798) [17] using FuGENE HD Transfection Reagent (Roche, Mississauga, ON) as per manufacturer's protocol. Following 24 hours, medium was removed and replaced with medium containing cisplatin for an additional 48 hours. The JNK inhibitor II (SP600125) and vorinostat were purchased from Calbiochem, Gibbstown, NJ.

3-(4,5-Dimethylthiazol-2-yl)-2,5-Diphenyltetrazolium bromide (MTT) Assay

In 96-well flat-bottom plates (Costar, Corning, NY), 5000 cells/150 μl of cell suspension were used to seed each well. Cells were incubated overnight to allow for cell attachment and recovery and assayed for MTT activity following drug treatments. For analysis, 50 μl of a 5-mg/ml solution of the MTT tetrazolium substrate (Sigma) in phosphate-buffered saline was added and incubated for up to 6 hours at 37°C. The resulting violet formazan precipitate was solubilized by the addition of 100 μl of 0.01 M HCl in 10% SDS (Sigma-Aldrich, St. Louis, MO) solution shaking overnight at 37°C. The plates were then analyzed on a microplate reader (Synergy Mx Monochromator-Based Multi-Mode Microplate Reader) using Gen5 software, both from Biotek Instruments (Winooski, VT), at 570 nm to determine the optical density of the samples.

Transcriptome Analysis (RNA Sequencing)

Total RNA was isolated employing the RNeasy Isolation Kit (Qiagen, Frederick, MD). Messenger RNA expression profiling was performed using NuGen reagents (www.nugeninc.com). After amplification, libraries compatible with Illumina NGS methods were prepared using the Ovation Ultra Low Library Prep Kit (NuGen). The quality of each library was assessed using a Bioanalyzer 2100 (Agilent Technologies). Kappa Library Quant Kits (KappaBiosystems; www.kapabiosystems.com) were used for library quantitation. Cluster generation and 2 × 36 bp paired-end sequencing was performed over a single lane using the Illumina GAIIx or HiSeq Genome Analyzer workstation. The RNA-Seq data were analyzed and quantified employing Cufflinks [18].

Western Blot Analysis

Cells plated at 0.7×10^6/60-mm dish were incubated overnight and treated with the indicated drug for 24 hours. Protein samples were collected in RIPA buffer (50 mM Tris-CL pH 7.5, 150 mM sodium chloride, 1 mM EDTA, 1% Triton-X-100, 0.25% sodium deoxycholate, 0.1% SDS) containing the protease inhibitors 50 mM sodium fluoride, 1 mM sodium orthovanadate, 10 mM β-glycerolphosphate, and 1× Protease Inhibitor Cocktail

(Sigma). Protein concentrations were determined using Bio-Rad Protein Assay (Mississauga, Ontario, Canada) and a Biomate 3 Spectrophotometer (Thermo Fisher Scientific, Waltham, MA). The Western blot methodology employed was previously described [19]. Antibodies specific for ATF3 were purchased from Santa Cruz Biotechnology (Santa Cruz, CA); Actin from Sigma; and ERK, phospho-ERK (Tyr204), Jun, phospho-Jun (Ser73), Hsp27, and phospho-hsp27 (Ser78) from Cell Signaling Technology (Beverly, MA). Visualization of protein bands was performed using the Supersignal West Pico Chemiluminescent Substrate (Pierce, Rockford, IL) and developed using the Syngene Bio-Imaging System (Syngene, Frederick, MD).

Quantitative Reverse Transcriptase Polymerase Chain Reaction (Q-RT-PCR)

Cells plated at 0.8×10^6 cells per 10-cm dish were incubated at 37°C overnight and then treated with cisplatin for 24 hours. Total RNA was extracted from cell samples using the RNAeasy kit (Qiagen). RNA concentrations were quantified using a NanoDrop ND-1000 spectrophotometer (Wilmington, DE). One microgram of total RNA was reverse-transcribed to complementary DNA for Q-RT-PCR as previously described [20]. The Applied Biosystems AB 7500 Real-Time PCR system (Applied Biosystems, Foster City, CA) was used to detect amplification. A real-time PCR was carried out employing Taq Man Gene Expression Assay Primer/Probe (Applied Biosystems, ATF3, HS00231069) and the housekeeping gene human GAPDH (20×) (Applied Biosystems, HS4333764-F) as per manufacturer's instructions. Three independent experiments were performed to determine the average gene expression and standard deviation.

Patient tumor tissue and matched adjacent normal lung tissue from at least 10 cm from the tumor were collected upon resection (lobectomy) and similarly evaluated (Ottawa Hospital Research Ethics Board; Protocol # 20120559-01H). Areas containing tumor were identified by routine gross pathological examinations. Cores of approximately 2 mm were obtained using a sterile biopsy punch that were further sliced with a scalpel to obtain approximately 2 × 2 × 1 mm tumor slices. The slices were randomized, and three slices were placed into each well of a 24-well plate and cultured in Dulbecco's modified Eagle's medium (HyClone) supplemented with 10% heat-inactivated FBS (Medicorp) and 100 U/ml antibiotic/antimycotic solution (Sigma). After 48-hour drug treatments, the tumor slices were processed for RNA extraction and RT-PCR analysis of ATF3 mRNA levels as described above in triplicate.

High-Throughput Chemical Library Screen

Wild-type and ATF3−/− MEFs cells were treated with a chemical library of 1200 FDA-approved compounds (Prestwick Chemical, Illkirch, France) [21]. All compounds were supplied in a 10-mM stock diluted in DMSO and were used at a final concentration of 5 μM. Cytotoxicity was evaluated for the drug library for each cell line employing the MTT assay; a greater than 20% difference in response in the wild type versus the ATF3−/− MEFs was considered a "hit." A second screen was then performed in Calu6 cells pretreated with the drug library at 1 μM for 24 hours and then for an additional 48 hours with or without 0.4 μg/ml of cisplatin. In this case, cytotoxicity was evaluated for the drug library alone, cisplatin treatment alone, and each combination, and a greater than 20% difference in response in the combination compared to either agent alone was considered a "hit."

Statistical Analyses

Significance between MTT viability curves was determined by one-way analysis of variance employing Bonferroni's multiple comparison test, whereas evaluations between columns was performed employing a two-way analysis of variance Bonferroni's multiple-comparison test. The combination effect of vorinostat and cisplatin was calculated using CalcuSyn computer software (Biosoft, Cambridge, UK). Combination index (CI) values were graphed on fraction affected-CI (Fa-CI) plots. A CI < 1 is a synergistic interaction, CI = 1 is additive, and CI > 1 is antagonistic.

Results

Derivation of Cisplatin-Resistant NSCLC Sublines

In this study, we developed a series of cisplatin-resistant clones from the Calu6 and H23 NSCLC cell lines (designated Calu6cisR1-3 and H23cisR1-3, respectively). Both parental cell lines are derived from NSCLC adenocarcinomas and show genetic mutations in KRAS and p53, common to this tumor type [22,23]. To derive Calu6 and H23 sublines resistant to cisplatin, cells were plated and treated with 2 μg/ml of cisplatin until a surviving fraction of about 10^{-6} remained [16]. Surviving colonies were then isolated and propagated for more than 20 population doublings in the absence of cisplatin. Their responsiveness to cisplatin, carboplatin, and the anthracycline doxorubicin (an intercalating DNA-damaging agent [24], employed as a comparator) was determined by the MTT Cell Viability Assay following 48 hours of treatment (Figure 1*A*). The cisplatin and carboplatin treatments followed a similar pattern, with all three resistant cisR sublines demonstrating significantly less cytotoxicity. The Calu6cisR sublines demonstrated more variability in their responses, whereas the H23cisR sublines showed a more consistent and reduced cytotoxic response to cisplatin and carboplatin. The resistant phenotype was restricted to platins, as all of the resistant clones with the exception of Calu6cisR3 showed similar cytotoxicity to their parental counterparts in response to doxorubicin (Figure 1*A*).

To further characterize these cisplatin-resistant sublines, we determined their proliferation rate measured by trypan blue exclusion cell counts, with measurements carried out over 200 hours in culture. The H23 parental and their cisR sublines (data not shown) showed similar doubling time kinetics. However, the Calu6cisR sublines, demonstrating similar cellular morphology to their parental counterparts (Figure 1*B*), displayed a significantly lower rate of proliferation as assessed by their doubling time. The slow growth of Calu6cisR3 correlates with its enhanced resistance to the above agents. Following the assessment of their growth kinetics, we focused our subsequent experiments on comparing Calu6 versus Calu6cisR1 and H23 versus H23cisR1.

Differential Induction of ATF3 in Cisplatin-Sensitive NSCLC Cells

Differentially expressed genes between cells sensitive or resistant to cisplatin following treatment may identify key regulators driving the tumor cell–induced cytotoxicity of this important clinical agent. To identify such differentially regulated genes, we compared cisplatin-sensitive parental lines Calu6 and H23 to their representative matching resistant sublines Calu6cisR1 and H23cisR1 by performing RNA-seq full transcriptome analysis. We compared expression levels of each parental line to its paired cisR1 resistant subline treated with cisplatin (2 μg/ml, 24 hours). We focused on differentially expressed genes that were cisplatin dependent, limiting

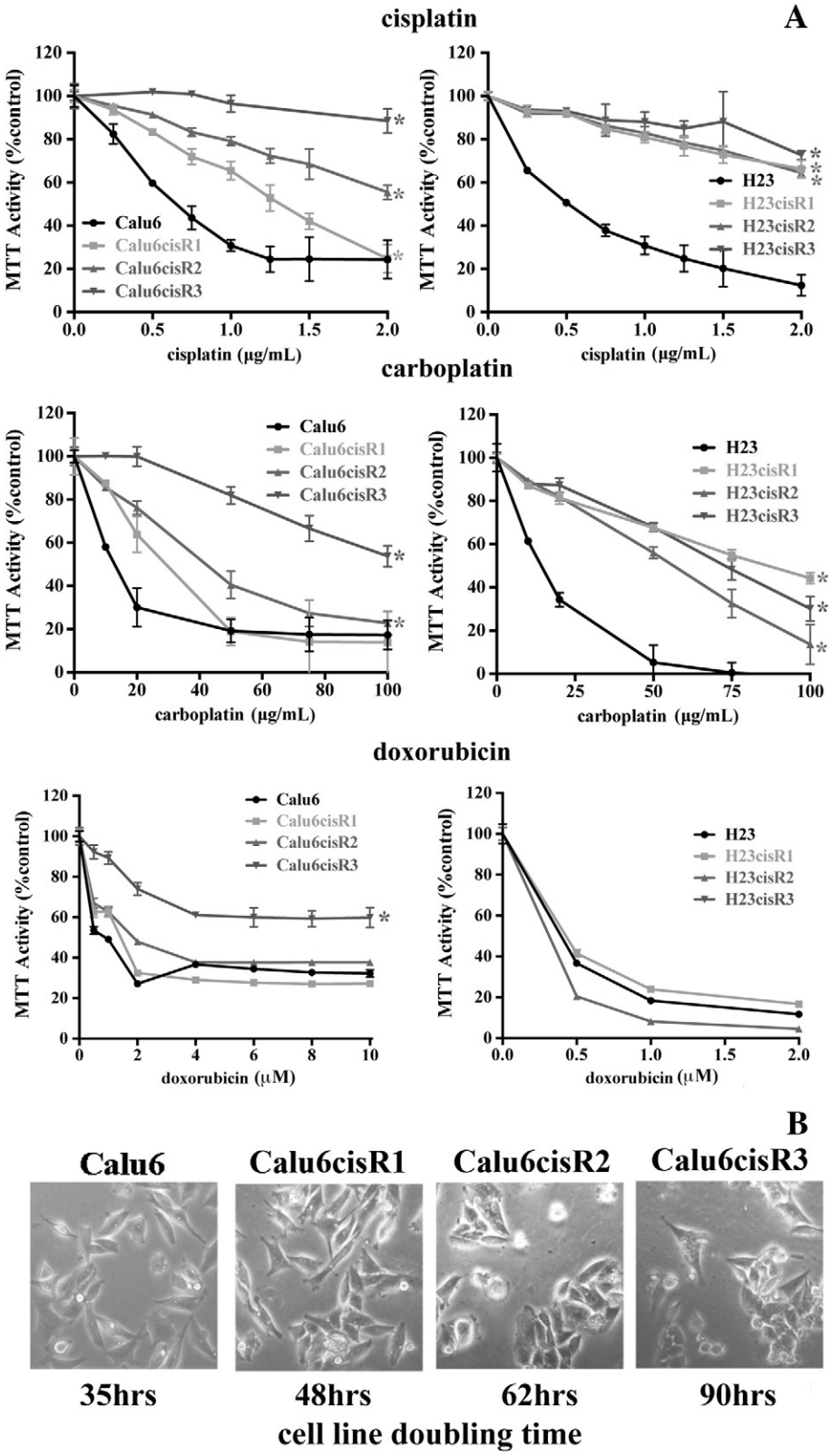

Figure 1. (A) MTT analysis of Calu6, Calu6cisR1-3, H23, and H23cisR1-3 following 48-hour treatments with cisplatin, carboplatin, and doxorubicin. Cisplatin and carboplatin treatments showed reduced cytotoxicity in the Calu6cisR1-3 and H23cisR1 compared to their parental cell lines. With the exception of Calu6cisR3, response to doxorubicin treatment was similar in the parental and cisR1 sublines. *Significant difference in the viability curves of the cisR sublines compared to their parental counterparts ($P < .05$). (B) No significant morphological differences were observed between the parental and resistant sublines (phase microscopy); however, proliferation rates as determined by cell doubling times were reduced in the Calu6cisR sublines, and this was most pronounced in the Calu6cisR3 cell line.

our analysis to only cisplatin-treated cells. The RNA-seq analysis was performed by StemCore (Ottawa Hospital Research Institute) using an Illumina GAIIx platform [25,26] generating 40 million sequencing reads per sample with 89% to 90% of reads mapping back to the genome. In the Calu6 versus Calu6cisR1 cells, 932 genes were differentially expressed, whereas in the H23 versus H23cisR1-cells, 601 genes were differentially expressed (Log_2> ±2). A total of 42 differentially induced genes were identified that were common to both cell lines (Figure 2*A*).

Exploring the top differentially expressed genes (top five shown in Supplemental Table 1), we found ATF3 to be the most significantly upregulated gene in both parental cell lines compared to their cisR1 sublines (Figure 2*B*). We further expanded on these results to determine the levels of ATF3 expression following the cytotoxic dose of 4 μg/ml of cisplatin for up to 24 hours in the Calu6 cell line and all three of its respective resistant sublines. Employing Q-RT-PCR, the differential induction of ATF3 following cisplatin treatment is clearly demonstrated, as only the Calu6 parental line showed significant ATF3 expression. ATF3 mRNA was induced in a time-dependant fashion, requiring at least 12 hours to become clearly evident (Figure 2*C*). Western blot analyses of both the Calu6 and the H23 and their derived cisR1-3 sublines demonstrated that significant induction of ATF3 by cisplatin treatment (4 μg/ml, 24 hours) is specific to the sensitive parental lines compared to their resistant cisR sublines (Figure 2*D*).

Cisplatin Induces ATF3 Expression in Ex Vivo NSCLC Tumors

To determine the ability of cisplatin to induce ATF3 expression in patient-derived NSCLC tissue as a more relevant clinical model, we evaluated *ex vivo* tissue samples from patients undergoing surgery for NSCLC. Tumor tissue and adjacent normal controls from six NSCLC patients were assayed for ATF3 expression employing Q-RT-PCR following 48 hours of treatment. ATF3 induction of greater than five-fold (normal untreated tissue used to normalize in all cases) was considered as a significant induction that is in line with our cell-line data. In all of the six patient tissues evaluated, the normal lung tissue failed to significantly induce ATF3 (Figure 3). In the tumor tissues, three of six showed significant ATF3 induction following cisplatin treatment. This is the first report of the ability of cisplatin to induce ATF3 directly in tumor tissue.

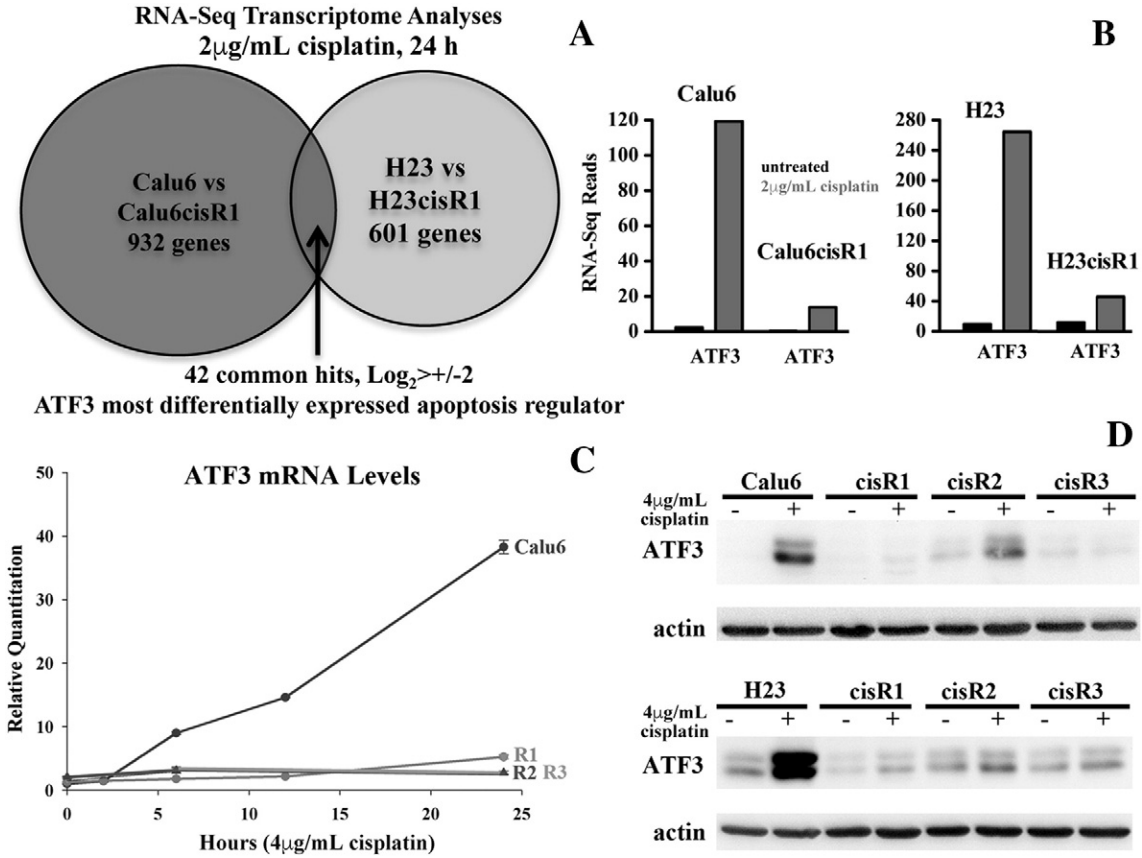

Figure 2. (A) RNA-seq analysis of Calu6 and H23 parental versus their respective cisR1 resistant clones identified 42 commonly differentially expressed genes in both cell lines following 2-μg/ml cisplatin treatment for 24 hours. (B) The cellular stress response gene ATF3 was differentially induced in cisplatin-treated sensitive parental lines but not their cisR1 sublines as indicated by the RNA-seq reads determined in this analysis (2-μg/ml cisplatin treatments for 24 hours). (C) Q-RT-PCR confirmed and expanded upon the differential expression of ATF3 in cisplatin-treated Calu6 cells compared to their Calu6cisR1-3 cisplatin-resistant sublines following the cytotoxic 4-μg/ml treatments of cisplatin for up to 24 hours. (D) Western blot analysis of ATF3 expression in cisplatin-treated Calu6 and H23 parental cell lines compared to their Calu6cisR1-3 and H23cisR1-3 cisplatin-resistant sublines following the cytotoxic 4-μg/ml treatments of cisplatin for 24 hours.

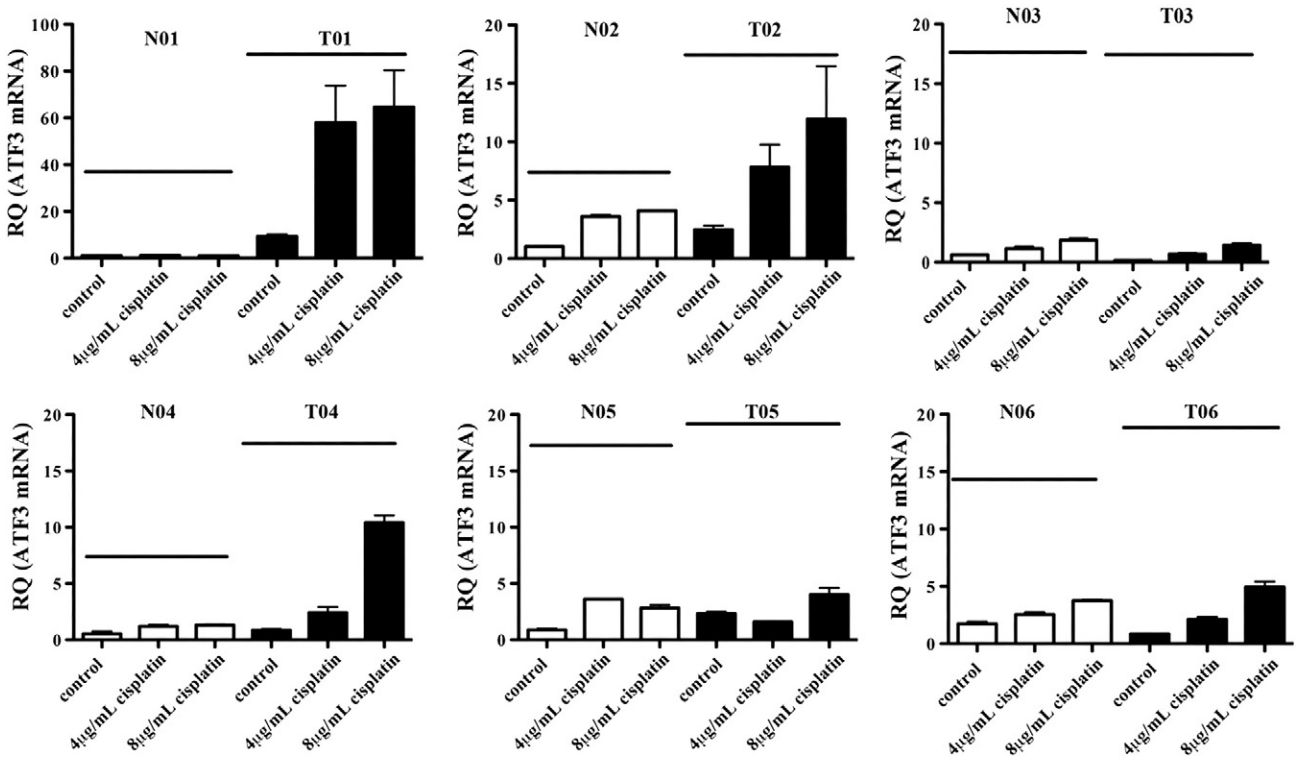

Figure 3. Levels of ATF3 mRNA following solvent or cisplatin treatments (0, 4, and 8 μg/ml) for 48 hours in six NSCLC (T) and adjacent normal (N) *ex vivo* tissues. Cisplatin-induced expression of greater than five-fold was observed in three of six NSCLC tissue samples evaluated but in none (0/6) of the normal adjacent tissues evaluated.

JNK Activation Regulates Cisplatin-Induced ATF3 Expression

Because previous studies have demonstrated that MAPKinases can regulate cisplatin-induced cytotoxicity [13] as well as ATF3 expression [15], we evaluated the status and activation of the JNK (assayed by evaluating the phosphorylation of its target c-jun [27]), ERK (assayed by phopho-ERK levels), and p38 (assayed by evaluating the phosphorylation of its target HSP27 [28]) following similar 4-μg/ml cisplatin treatments in Calu6 and Calu6cisR1 and in H23 and H23cisR1 (Figure 4*A*). In both cases, the parental cells showed significant JNK activation in a time-dependant manner. JNK activation was pronounced by 12 hours of treatment while lacking in both resistant cisR1 sublines. Significant activation of the ERK and p38 pathways was not readily detected either in the parental NSCLC cell lines or in their resistant sublines following cisplatin treatments (Figure 4*A*). To determine if the observed JNK activation mirrored the induction pattern of ATF3 as well, we performed a dose- and time-dependant assessment of ATF3 expression and p-c-jun induction in both parental cell lines (Supplemental Figure 1). Calu6 and H23 cells were treated with 0, 1, 2, and 4 μg/ml of cisplatin for 12, 24, and 36 hours and evaluated for ATF3 expression and phosphorylation levels of c-jun. In both cell lines, ATF3 was induced in a time- and dose-dependent manner. This expression pattern closely mirrored the phosphorylation levels of c-jun induced by cisplatin treatments (Supplemental Figure 1).

To expand on these findings, we evaluated ATF3 and phosphorylated c-jun levels following 24-hour cisplatin treatments (0-8 μg/ml) in the breast cancer cell lines MCF7 and T47D and in the prostate cancer–derived cell lines LNCAP and PC3 (Supplemental Figure 1). Similarly, ATF3 was induced in a dose-dependent manner in all four cell lines tested. These expression levels also closely mirrored cisplatin-induced phosphorylation of c-jun and were in line with previously published studies [14,15,19]. To determine the role of JNK activity in both cisplatin resistance and lack of ATF3 induction, we treated Calu6 with 10 μM of the JNK inhibitor SP600125 in combination with 1 and 4 μg/ml of cisplatin for 48 hours. Cells treated with the JNK inhibitor were less responsive to cisplatin-induced cytotoxicity (Figure 4*B*). In the Calu6cisR1 subline, expression of a hyperactive JNK construct [17] enhanced cisplatin-induced cytotoxicity, as assessed by the MTT cell viability assay (Figure 4*C*). Expression of the hyperactive JNK had no impact on cytotoxicity in the absence of cisplatin exposure. Furthermore, active JNK rescued cisplatin-induced ATF3 expression in the Calu6cisR1 subline, as assessed by Western blot analysis (Figure 4*D*).

ATF3 Induction by DNA Damaging Agents

To determine the role that ATF3 plays in regulating the cytotoxicity of a variety of chemotherapeutic agents, we evaluated the cytotoxic effects of these agents in ATF3 null (–/–) cells and their respective wild-type MEF counterparts. Evaluated agents included cisplatin, carboplatin, doxorubicin, and docetaxel that targets tubulin cytoskeleton and acts as a mitotic poison [29] (Figure 4*A*). MTT cell viability assays demonstrated ATF3–/– MEFs to be resistant to cisplatin, carboplatin, and doxorubicin, but there was no difference in sensitivity to docetaxel (Figure 5*A*).

We further evaluated the sensitivity of the Calu6 and H23 cell lines and their respective resistant subline (cisR1) to docetaxel treatment as above and showed no differential sensitivity between the parental and cisR1 sublines (Figure 5*B*). The other three agents' sensitivities were

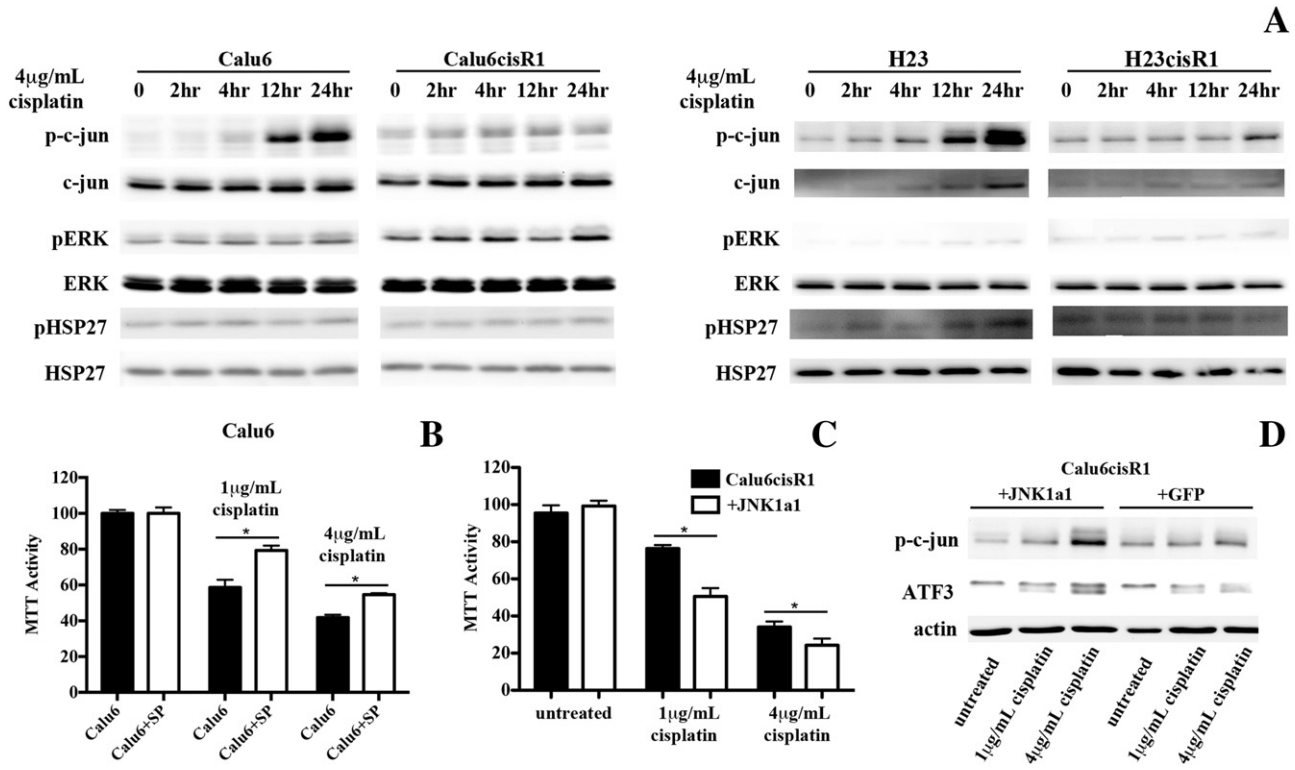

Figure 4. (A) Following 4-μg/ml cisplatin treatments for up to 24 hours, Western blot analysis showed differential induction of JNK MAPKinase activation (through phosphorylated c-jun) but not ERK (phospho-ERK) or p38 (through phosphorylated HSP27) in both Calu6 and H23 cells. This induction was abrogated in their respective cisR1 sublines. (B) MTT analysis of Calu6 cells following 48-hour treatments of (0, 1, and 4 μg/ml) cisplatin with or without 10-μM treatment of the JNK inhibitor SP600125. *Significant differences between columns highlighted (P< .05). (C) Exogenous expression of a JNK-activated construct enhanced cisplatin cytotoxicity in the Calu6cisR1 subline as assessed by MTT cell viability assay following 48-hour cisplatin treatments. *P< .05 between columns highlighted. (D) Exogenous expression of activated JNK in Calu6cisR1 also rescued cisplatin-inducible ATF3 expression in these cells assessed by Western blot analysis (24-hour treatments).

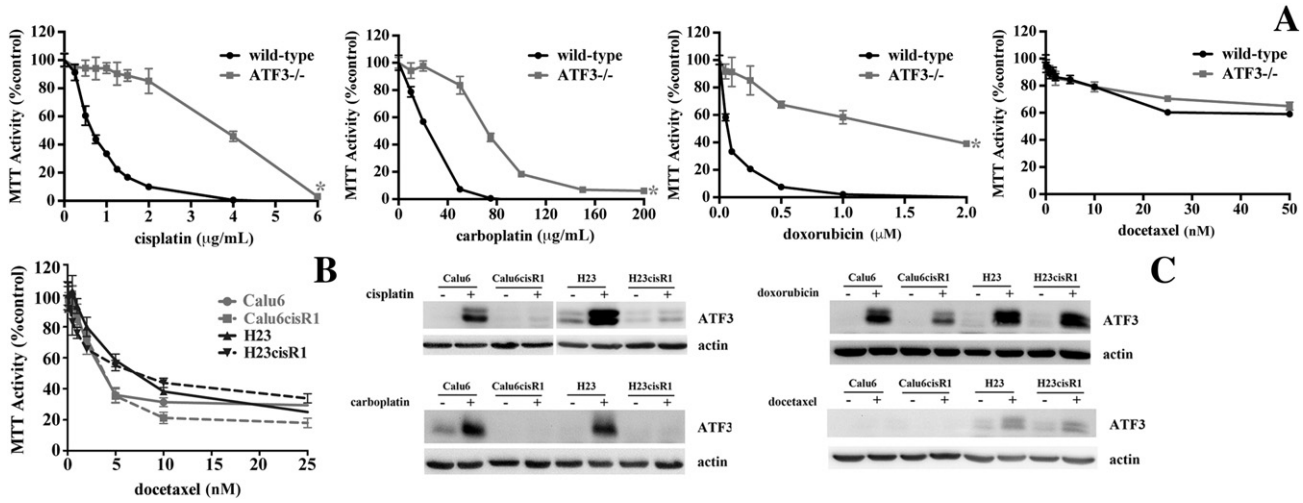

Figure 5. (A) MTT analysis of wild-type and ATF3−/− MEFs following 48-hour treatments of cisplatin, carboplatin, doxorubicin, and docetaxel. Loss of ATF3 inhibits cisplatin-, carboplatin-, and doxorubicin-induced cytotoxicity but had no effect on docetaxel cytotoxicity. *Significant difference in the viability curves comparing the wild-type and the ATF3−/− MEFs responses (P< .05). (B) MTT analysis of Calu6, Calu6cisR1, H23, and H23cisR1 following 48-hour treatments with docetaxel showing no significant differences in sensitivity (note: cisplatin, carboplatin, and doxorubicin treatments were presented in Figure 1*A*). (C) Western blot analysis shows significant ATF3 induction restricted to the parental cell lines with cisplatin and carboplatin treatments. Doxorubicin treatments showed similar ATF3 induction in both the parental and their cisR1 sublines. No significant ATF3 induction was observed with the docetaxel treatments in any of the lines tested, with a weak induction in the H23 series (24-hour treatments, IC50 dose).

displayed in Figure 1. When evaluating ATF3 expression levels following treatments (IC50 concentrations employed for 24 hours), differential ATF3 expression following carboplatin treatments was observed in a similar pattern to cisplatin (Figure 5*C*). Doxorubicin was also a potent inducer of ATF3; however, unlike the platins, both the parental and the resistant sublines readily induced ATF3. Furthermore, ATF3 was not readily induced with weak induction in the H23 and H23cisR1 in the docetaxel-treated cells even with similar levels of cell cytotoxicity observed (Figure 5*C*).

Inducers of ATF3 Enhance Cisplatin Cytotoxicity

We aimed to examine whether inducers of ATF3 expression can enhance the cytotoxicity of cisplatin. A high-throughput drug screen to identify agents whose cytotoxicity was ATF3 dependent was conducted. Both wild-type (ATF3+/+) and null ATF3−/− MEFs were treated with a chemical library of 1200 FDA-approved compounds at 5 μM for 48 hours (Supplemental Table 2a). We identified 41 agents that displayed a greater than 20% cytotoxicity in the ATF3+/+ compared to the ATF3−/− MEFs (less than a 2% "hit" rate), indicating a level of specificity to this approach, including the identification of three agents that we have shown to be ATF3 inducers in our previous work [30–32]. A secondary screen with the Calu6 cell line used 1-μM library pretreatments for 24 hours followed by 0.4-μg/ml cisplatin treatment or no treatment for an additional 48 hours. In this screen, 12 agents were identified with at least a 20% higher cytotoxicity in the combination treatment than either the library and cisplatin treatments alone (Supplemental Table 2b).

Of interest, vorinostat was identified in both library screens and was previously shown to enhance cisplatin responsiveness [32,33]; however, the mechanism of action of this phenomenon has not been determined. We first confirmed the differential sensitivity of the wild-type and ATF3−/− MEFs to vorinostat treatments employing 0- to 10-μM treatments for 48 hours (Figure 6*A*), clearly demonstrating a role for ATF3 in regulating vorinostat cytotoxicity. Employing these MEFs cell lines, we also demonstrated that the enhanced cytotoxicity of 24-hour pretreatment with either 1 or 2 μM vorinostat with cisplatin (further 48 hours) was dependant on ATF3 as significant cytotoxicity was observed only in the wild-type but not the ATF3−/− deficient MEFs (Figure 6*B*). In the NSCLC cells, similar to their resistance to cisplatin, H23cisR1 showed a more robust resistance to vorinostat than Calu6cisR1 when compared to their parental lines (Figure 6*C*). Vorinostat is a potent inducer of ATF3 in both the Calu6 and H23 cells with an attenuated but discernable response in the cisR1 cells following 24 hours of treatment (Figure 6*D*). In both the parental Calu6 and H23 cells and their cisR1 derivatives, vorinostat enhanced the cytotoxicity of cisplatin (0-, 1-, 2-, or 5-μM 24-hour vorinostat pretreatment followed by 48 hours of cisplatin in combination with vorinostat) as determined by MTT analysis (Figure 6, *E* and *F*). This combination generally induced synergistic cytotoxicity, particularly at the 2-μM vorinostat concentration, as determined by CI evaluation, even within the cisR1 sublines (Supplemental Figure 2). Furthermore, in the Calu6cisR1 and H23cisR1sublines, 24-hour treatments with 5 μM vorinostat followed by 24-hour treatment with either 2 or 4 μg/ml of cisplatin showed enhanced ATF3 induction in the combination treatments (Figure 6*G*). This suggests a potential role for ATF3 expression in overcoming cisplatin resistance that requires further study.

Discussion

Lung cancer, predominantly NSCLC, is the most common cause of death from cancer worldwide [1]. The platins cisplatin and carboplatin are among the most active agents, with platin combination chemotherapy typically the first-line therapy in advanced disease. Nonetheless, benefit is limited, with few patients remaining progression free at 5 years [2]. New combinations of platins with novel agents are urgently required [4]. The mechanisms regulating platin cytotoxicity are currently poorly understood [7,34], and understanding these mechanisms could suggest 1) rational strategies strategies to enhance their efficacy and 2) clinically useful predictive biomarkers of platin response.

In this study, we established a number of cisplatin-induced resistant clones (cisR) in the Calu6 and H23 NSCLC-derived cell lines. Employing RNA-seq analyses, we identified ATF3 expression as a highly significant cisplatin differentially induced gene in the sensitive parental lines Calu6 and H23 compared to their cisplatin-resistant counterparts. The ability of cisplatin to induce ATF3 was also demonstrated in a cohort of NSCLC surgically excised NSCLC tissue *ex vivo* but not in their adjacent normal lung tissue. The MAPKinase pathways play a significant role in regulating both cisplatin cytotoxicity and ATF3 expression [9,19,35]. Cisplatin-induced MAPKinase activation, specifically activation of the JNK pathway, was abrogated in Calu6cisR1 and H23cisR1 cells. Furthermore, expression of activated JNK enhanced cisplatin cytotoxicity and ATF3 expression in the Calu6cisR1 resistant subline. Furthermore, MEFs deficient in ATF3 were resistant to cisplatin and carboplatin but not to the tubulin stabilizer docetaxel compared to their wild-type counterparts. The inability to induce ATF3 may represent a novel mechanism of cisplatin resistance that requires further study. The small molecule library screens performed in this study provide initial evidence that ATF3 activating agents can be identified that enhance cisplatin response in both the sensitive parental Calu6 and H23 cell lines but importantly also in their respective cisR1 sublines. The HDAC inhibitor vorinostat was identified in this study as an agent that both enhanced cisplatin cytotoxicity in Calu6 cells but whose cytotoxicity was also regulated in part by ATF3 in a subsequent screen comparing the cytotoxicity of the same FDA-approved 1200 drugs in wild-type compared to ATF3−/− deficient cells. Of the 1200 agents evaluated, only 41 showed significant differential cytotoxicity between wild-type and ATF3−/− deficient MEFs, indicating that there is specificity in the requirement for ATF3-induced cytotoxicity. However, HDAC inhibitors like vorinostat do not show specificity and affect multiple signaling pathways [36,37], and although these drugs demonstrate preclinical and clinical activity in combination with platins in NSCLC, off-target toxicities limited their utilization [38]. These data provide the rationale that ATF3 is a therapeutic target and the identification of novel and more specific enhancers of ATF3 may provide a novel strategy for development of next-generation platin-combination therapies.

With 30% to 50% of patients presenting with high-level intrinsic platin resistance [39], development of reliable predictive markers of platin response in NSCLC is also urgently needed. The markers or gene signatures that have previously been explored relied on the assessment of gene expression in archival or pretreatment patient tumor samples, where tumor heterogeneity and instability of potential biomarkers limit their reliability [40]. This is in contrast to the predictive markers employed for EGFR and ALK targeted agents, where the presence of EGFR mutations and ALK

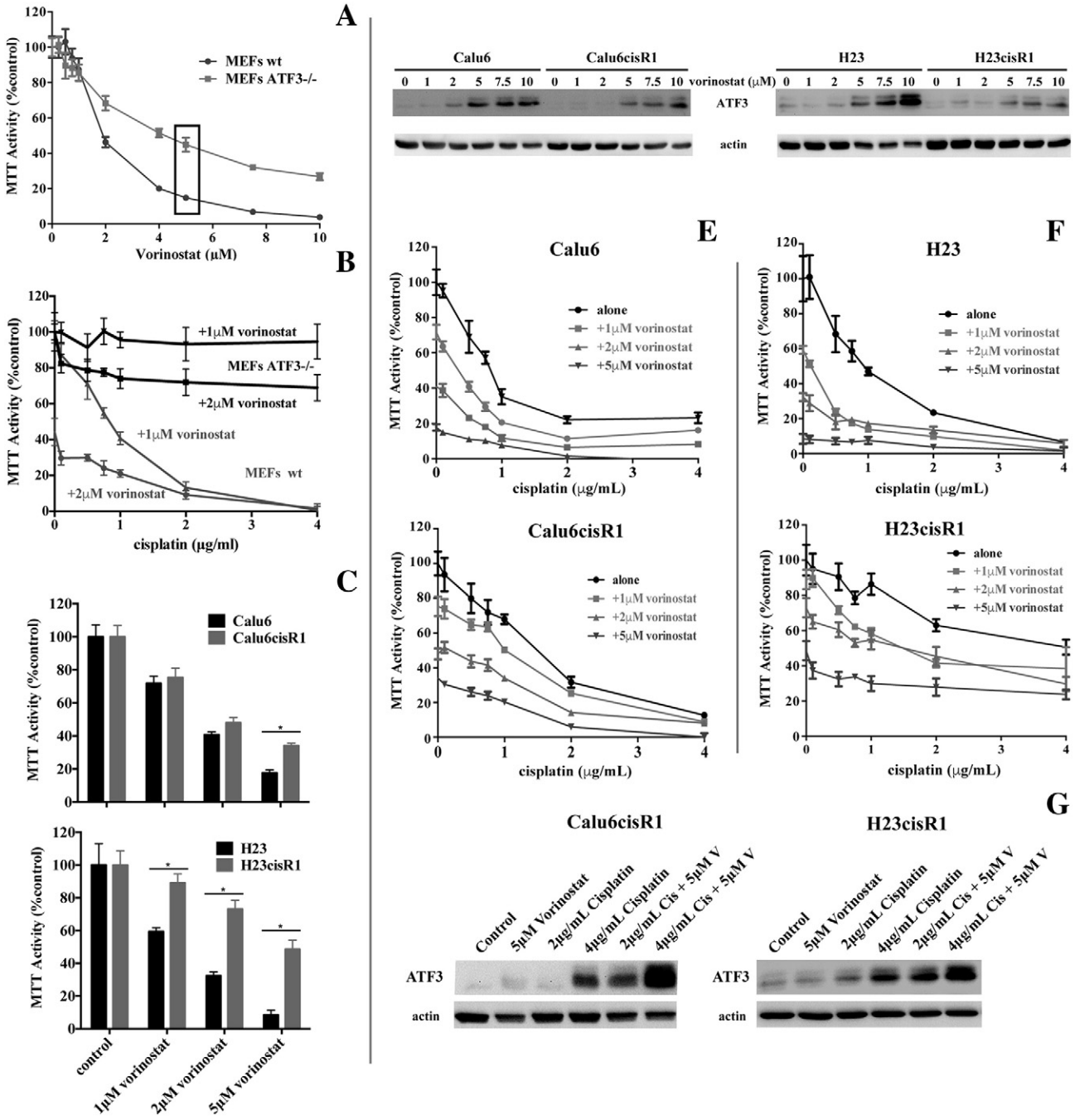

Figure 6. (A) MTT analysis of wild-type and ATF3−/− MEFs following 48-hour treatments with vorinostat showing that loss of ATF3 inhibits vorinostat-induced cytotoxicity in MEFs. (B), MTT analysis of wild-type (wt) and ATF3−/− deficient MEFs following 24-hour pretreatments of 1 and 2 μM vorinostat followed by cisplatin treatment in combination for a further 48 hours. Enhanced cytotoxicity with the combination was observed only in the wild-type MEFs. (C) MTT analysis comparing response of Calu6 to Calu6cisR1 and H23 to H23cisR1 following 0-, 1-, 2-, and 5-μM vorinostat treatment for 72 hours. The H23cisR1 showed significant resistance to vorinostat. *Significant differences between columns highlighted (P< .05). (D) Western blot analysis shows ATF3 induced by vorinostat treatments (0-10 μM, 48 hours) in the Calu6 and the H23 parental lines that was evident but attenuated in their cisR1 sublines. (E) MTT analysis of Calu6 and Calu6cisR1 and (F) H23 and H23cisR1 following 24-hour pretreatments of 0, 1, 5, and 5 μM vorinostat followed by cisplatin treatment in combination for a further 48 hours. Enhanced cytotoxicity with the combination was observed in all four lines compared to either agent alone. (G) Western blot analysis shows ATF3 induced by 2- and 4-mg/ml cisplatin treatment (24 hours) was enhanced by vorinostat treatment (5 μM, 24-hour pretreatment) in the Calu6cisR1 and the H23cisR1 resistant sublines.

translocations, respectively, is a robust predictor of response [41,42]. A similar absence/presence marker associated with platin response would represent a similar ideal predictive biomarker. Low basal levels of ATF3 in all the cell lines and sublines evaluated, as well as in untreated normal and tumor tissue, was in contrast to the significant induction of ATF3 seen specifically in sensitive parental cell lines and in a cohort of resected NSCLC surgical samples. This expression profile suggests its potential as a treatment-induced biomarker of

platin responsiveness. The feasibility of this approach was demonstrated in this study as cisplatin induction of ATF3 (as assessed by Q-RT-PCR) was observed in three of six tumor tissues but not in the six normal tissues evaluated. These data demonstrate the ability to rapidly evaluate ATF3 expression in *ex vivo* tissue samples within a clinically relevant time window (72 hours in our study). We plan further assessment of *ex vivo* ATF3 induction in NSCLC patients undergoing treatment with platin-based regimens to determine if it is a useful predictive biomarker of clinical response to platins.

Supplementary data to this article can be found online at http://dx.doi.org/10.1016/j.neo.2016.07.004.

Acknowledgements

We thank the team at StemCore (Ottawa Hospital Research Institute) including Pearl Campbell as well as Ivan Gorn, Jennifer E. L. Hanson, and Stephanie Reid for expert technical assistance. The support of the surgeons in the Division of Thoracic Surgery at the Ottawa Hospital (Drs. Sebastien Gilbert, Donna Maziak, Andrew Seely, Farid Shamji, and Sudhir Sundaresan) has been instrumental in procuring human tumor tissues.

References

[1] Abratt RP and Hart GJ (2006). 10-year update on chemotherapy for non–small cell lung cancer. *Ann Oncol* **17**(Suppl 5), v33–v36.
[2] Kelland L (2007). The resurgence of platinum-based cancer chemotherapy. *Nat Rev Cancer* **7**, 573–584.
[3] Di Maio M, Chiodini P, Georgoulias V, Hatzidaki D, Takeda K, Wachters FM, Gebbia V, Smit EF, Morabito A, and Gallo C, et al (2009). Meta-analysis of single-agent chemotherapy compared with combination chemotherapy as second-line treatment of advanced non–small-cell lung cancer. *J Clin Oncol Off J Am Soc Clin Oncol* **27**, 1836–1843.
[4] Souquet PJ, Chauvin F, Boissel JP, and Bernard JP (1995). Meta-analysis of randomised trials of systemic chemotherapy versus supportive treatment in non-resectable non–small cell lung cancer. *Lung Cancer* **12**(Suppl 1), S147–S154.
[5] Seve P and Dumontet C (2005). Chemoresistance in non–small cell lung cancer. *Curr Med Chem Anticancer Agents* **5**, 73–88.
[6] Stewart DJ (2007). Mechanisms of resistance to cisplatin and carboplatin. *Crit Rev Oncol Hematol* **63**, 12–31.
[7] Siddik ZH (2003). Cisplatin: mode of cytotoxic action and molecular basis of resistance. *Oncogene* **22**, 7265–7279.
[8] Manic S, Gatti L, Carenini N, Fumagalli G, Zunino F, and Perego P (2003). Mechanisms controlling sensitivity to platinum complexes: role of p53 and DNA mismatch repair. *Curr Cancer Drug Targets* **3**, 21–29.
[9] Sedletska Y, Giraud-Panis MJ, and Malinge JM (2005). Cisplatin is a DNA-damaging antitumour compound triggering multifactorial biochemical responses in cancer cells: importance of apoptotic pathways. *Curr Med Chem Anticancer Agents* **5**, 251–265.
[10] Karin M and Gallagher E (2005). From JNK to pay dirt: jun kinases, their biochemistry, physiology and clinical importance. *IUBMB Life* **57**, 283–295.
[11] Sanchez-Prieto R, Rojas JM, Taya Y, and Gutkind JS (2000). A role for the p38 mitogen-activated protein kinase pathway in the transcriptional activation of p53 on genotoxic stress by chemotherapeutic agents. *Cancer Res* **60**, 2464–2472.
[12] Bragado P, Armesilla A, Silva A, and Porras A (2007). Apoptosis by cisplatin requires p53 mediated p38alpha MAPK activation through ROS generation. *Apoptosis* **12**, 1733–1742.
[13] Brozovic A and Osmak M (2007). Activation of mitogen-activated protein kinases by cisplatin and their role in cisplatin-resistance. *Cancer Lett* **251**, 1–16.
[14] Cai Y, Zhang C, Nawa T, Aso T, Tanaka M, Oshiro S, Ichijo H, and Kitajima S (2000). Homocysteine-responsive ATF3 gene expression in human vascular endothelial cells: activation of c-Jun NH(2)-terminal kinase and promoter response element. *Blood* **96**, 2140–2148.
[15] Lu D, Chen J, and Hai T (2007). The regulation of ATF3 gene expression by mitogen-activated protein kinases. *Biochem J* **401**, 559–567.
[16] Bar J, Gorn-Hondermann I, Moretto P, Perkins TJ, Niknejad N, Stewart DJ, Goss GD, and Dimitroulakos J (2015). miR profiling identifies cyclin-dependent kinase 6 downregulation as a potential mechanism of acquired cisplatin resistance in non–small-cell lung carcinoma. *Clin Lung Cancer* **16**, e121–e129.
[17] Derijard B, Hibi M, Wu IH, Barrett T, Su B, Deng T, Karin M, and Davis RJ (1994). JNK1: a protein kinase stimulated by UV light and Ha-Ras that binds and phosphorylates the c-Jun activation domain. *Cell* **76**, 1025–1037.
[18] Trapnell C, Roberts A, Goff L, Pertea G, Kim D, Kelley DR, Pimentel H, Salzberg SL, Rinn JL, and Pachter L (2012). Differential gene and transcript expression analysis of RNA-seq experiments with TopHat and Cufflinks. *Nat Protoc* **7**, 562–578.
[19] St Germain C, Niknejad N, Ma L, Garbuio K, Hai T, and Dimitroulakos J (2010). Cisplatin induces cytotoxicity through the mitogen-activated protein kinase pathways and activating transcription factor 3. *Neoplasia* **12**, 527–538.
[20] Kroupis C, Stathopoulou A, Zygalaki E, Ferekidou L, Talieri M, and Lianidou ES (2005). Development and applications of a real-time quantitative RT-PCR method (QRT-PCR) for BRCA1 mRNA. *Clin Biochem* **38**, 50–57.
[21] Wermuth CG (2004). Multitargeted drugs: the end of the "one-target-one-disease" philosophy? *Drug Discov Today* **9**, 826–827.
[22] Frese S, Brunner T, Gugger M, Uduehi A, and Schmid RA (2002). Enhancement of Apo2L/TRAIL (tumor necrosis factor–related apoptosis-inducing ligand)-induced apoptosis in non–small cell lung cancer cell lines by chemotherapeutic agents without correlation to the expression level of cellular protease caspase-8 inhibitory protein. *J Thorac Cardiovasc Surg* **123**, 168–174.
[23] Takahashi T, Carbone D, Takahashi T, Nau MM, Hida T, Linnoila I, Ueda R, and Minna JD (1992). Wild-type but not mutant p53 suppresses the growth of human lung cancer cells bearing multiple genetic lesions. *Cancer Res* **52**, 2340–2343.
[24] Havelka AM, Berndtsson M, Olofsson MH, Shoshan MC, and Linder S (2007). Mechanisms of action of DNA-damaging anticancer drugs in treatment of carcinomas: is acute apoptosis an "off-target" effect? *Mini-Rev Med Chem* **7**, 1035–1039.
[25] Tariq MA, Kim HJ, Jejelowo O, and Pourmand N (2011). Whole-transcriptome RNAseq analysis from minute amount of total RNA. *Nucleic Acids Res* **39**, e120.
[26] Wang Y, Mehta G, Mayani R, Lu J, Souaiaia T, Chen Y, Clark A, Yoon HJ, Wan L, and Evgrafov OV, et al (2011). RseqFlow: workflows for RNA-Seq data analysis. *Bioinformatics* **27**, 2598–2600.
[27] Levresse V, Marek L, Blumberg D, and Heasley LE (2002). Regulation of platinum-compound cytotoxicity by the c-Jun N-terminal kinase and c-Jun signaling pathway in small-cell lung cancer cells. *Mol Pharmacol* **62**, 689–697.
[28] Kostenko S, Johannessen M, and Moens U (2009). PKA-induced F-actin rearrangement requires phosphorylation of Hsp27 by the MAPKAP kinase MK5. *Cell Signal* **21**, 712–718.
[29] Muggia F and Kudlowitz D (2014). Novel taxanes. *Anticancer Drugs* **25**, 593–598.
[30] Dayekh K, Johnson-Obaseki S, Corsten M, Villeneuve PJ, Sekhon HS, Weberpals JI, and Dimitroulakos J (2014). Monensin inhibits epidermal growth factor receptor trafficking and activation: synergistic cytotoxicity in combination with EGFR inhibitors. *Mol Cancer Ther* **13**, 2559–2571.
[31] Niknejad N, Gorn-Hondermann I, Ma L, Zahr S, Johnson-Obeseki S, Corsten M, and Dimitroulakos J (2014). Lovastatin-induced apoptosis is mediated by activating transcription factor 3 and enhanced in combination with salubrinal. *Int J Cancer* **134**, 268–279.
[32] St Germain C, O'Brien A, and Dimitroulakos J (2010). Activating transcription factor 3 regulates in part the enhanced tumour cell cytotoxicity of the histone deacetylase inhibitor M344 and cisplatin in combination. *Cancer Cell Int* **10**, 32,1-11.
[33] Liu J, Edagawa M, Goshima H, Inoue M, Yagita H, Liu Z, and Kitajima S (2014). Role of ATF3 in synergistic cancer cell killing by a combination of HDAC inhibitors and agonistic anti-DR5 antibody through ER stress in human colon cancer cells. *Biochem Biophys Res Commun* **445**, 320–326.
[34] Takata R, Katagiri T, Kanehira M, Tsunoda T, Shuin T, Miki T, Namiki M, Kohri K, Matsushita Y, and Fujioka T, et al (2005). Predicting response to methotrexate, vinblastine, doxorubicin, and cisplatin neoadjuvant chemotherapy for bladder cancers through genome-wide gene expression profiling. *Clin Cancer Res* **11**, 2625–2636.
[35] Lu D, Wolfgang CD, and Hai T (2006). Activating transcription factor 3, a stress-inducible gene, suppresses Ras-stimulated tumorigenesis. *J Biol Chem* **281**, 10473–10481.
[36] Marks PA, Richon VM, and Rifkind RA (2000). Histone deacetylase inhibitors: inducers of differentiation or apoptosis of transformed cells. *J Natl Cancer Inst* **92**, 1210–1216.

[37] Ververis K, Hiong A, Karagiannis TC, and Licciardi PV (2013). Histone deacetylase inhibitors (HDACIs): multitargeted anticancer agents. *Biologics* **7**, 47–60.

[38] Owonikoko TK, Ramalingam SS, Kanterewicz B, Balius TE, Belani CP, and Hershberger PA (2010). Vorinostat increases carboplatin and paclitaxel activity in non–small-cell lung cancer cells. *Int J Cancer* **126**, 743–755.

[39] Schiller JH, Harrington D, Belani CP, Langer C, Sandler A, Krook J, Zhu J, Johnson DH, and Eastern Cooperative Oncology G (2002). Comparison of four chemotherapy regimens for advanced non–small-cell lung cancer. *N Engl J Med* **346**, 92–98.

[40] Souglakos J (2015). Customizing chemotherapy in non–small cell lung cancer: the promise is still unmet. *Transl Lung Cancer Res* **4**, 653–655.

[41] Aisner DL and Marshall CB (2012). Molecular pathology of non-small cell lung cancer: a practical guide. *Am J Clin Pathol* **138**, 332–346.

[42] Paez JG, Janne PA, Lee JC, Tracy S, Greulich H, Gabriel S, Herman P, Kaye FJ, Lindeman N, and Boggon TJ, et al (2004). EGFR mutations in lung cancer: correlation with clinical response to gefitinib therapy. *Science* **304**, 1497–1500.